

Mechanism of Catalytic Cyclohydroamination by Zirconium Salicyloxazoline Complexes

Laura E. N. Allan, Guy J. Clarkson, David J. Fox,* Andrew L. Gott, and Peter Scott*

Department of Chemistry, University of Warwick, Gibbet Hill Road, Coventry CV7 4AL, U.K.

Received July 25, 2010; E-mail: peter.scott@warwick.ac.uk

Abstract: The mechanism of hydroamination/cyclization of primary aminoalkenes by catalysts based on $\text{Cp}^*\text{LZr}(\text{NMe}_2)_2$ ($\text{L} = \kappa^2\text{-salicyloxazoline}$) is investigated in a range of kinetic, stoichiometric, and structural studies. The rate law is found to be $d[\text{substrate}]/dt = k[\text{catalyst}]^1[\text{substrate}]^0$ for all catalysts and aminoalkenes studied. The overall rate is similar for formation of five- and six-membered rings, and a substantial KIE ($k_{\text{H}}/k_{\text{D}}$) is observed, indicating the involvement of N–H bond-breaking in a rate-determining step (RDS) which is not ring-closure. Remarkably, the reaction proceeds at the same rate in THF as it does in toluene, but added non-cyclizable amine slows the reaction, indicating that while the metal is not acting as a Lewis acid in the RDS, the activated substrate is involved. Also in contrast to other catalysts, increasing steric bulk improves the rate, and the origins of this are investigated by X-ray crystallography. Thermodynamic parameters extracted from eight independent kinetic studies indicate moderate ordering ($\Delta S^\ddagger = -13$ to -23 cal/K·mol) and substantial overall bond disruption ($\Delta H^\ddagger = 17$ to 21 kcal/mol) in the rate-determining transition state. Secondary amines are unreactive, as is a catalyst with a single aminolizable site, thus excluding an amido mechanism. A catalytic cycle involving rate-determining formation of a reactive imido species is proposed. Stoichiometric steps in the process are shown to be feasible and have appropriate rates by synthetic and in situ NMR spectroscopic studies. The fate of the catalyst in the absence of excess amine (at the end of the catalytic reaction) is conversion to a metallacyclic species arising from CH activation of a peripheral substituent.

Introduction

Hydroamination, the addition of an N–H bond across an unsaturated C–C bond, is an atom-economical method for the efficient formation of N–C bonds and thus a topic of considerable interest.^{1–14} In particular, the enantioselective intramolecular cyclohydroamination of aminoalkenes has attracted much recent attention since chiral *N*-heterocycles have applications in the pharmaceutical and fine chemical industries.^{15–19} Pioneering studies by Marks in this area used chiral lanthanocene

complexes,^{20–25} which were followed some years later by non-cyclopentadienyl lanthanide catalysts.^{26–35} Recent interest has

- (1) Müller, T. E.; Beller, M. *Chem. Rev.* **1998**, *98*, 675.
- (2) Nobis, M.; Driessen-Hölscher, B. *Angew. Chem., Int. Ed.* **2001**, *40*, 3983.
- (3) Beller, M.; Breindl, C.; Eichberger, M.; Hartung, C. G.; Seayad, J.; Thiel, O. R.; Tillack, A.; Trauthwein, H. *Synth. Lett.* **2002**, *10*, 1579.
- (4) Pohlki, F.; Doye, S. *Chem. Soc. Rev.* **2003**, *32*, 104.
- (5) Hartwig, J. F. *Pure Appl. Chem.* **2004**, *76*, 507.
- (6) Hultsch, K. C. *Adv. Synth. Catal.* **2005**, *347*, 367.
- (7) Hultsch, K. C. *Org. Biomol. Chem.* **2005**, *3*, 1819.
- (8) Odom, A. L. *Dalton Trans.* **2005**, 225.
- (9) Aillaud, I.; Collin, J.; Hannedouche, J.; Schulz, E. *Dalton Trans.* **2007**, 5105.
- (10) Müller, T. E.; Hultsch, K. C.; Yus, M.; Foubelo, F.; Tada, M. *Chem. Rev.* **2008**, *108*, 3795.
- (11) Hegedus, L. S. *Angew. Chem., Int. Ed.* **1988**, *27*, 1113.
- (12) Hartwig, J. F. *Science* **2002**, *297*, 1653.
- (13) Beller, M.; Seayad, J.; Tillack, A.; Jiao, H. *Angew. Chem., Int. Ed.* **2004**, *43*, 3368.
- (14) Buffat, M. G. P. *Tetrahedron* **2004**, *60*, 1701.
- (15) Arredondo, V. M.; Tian, S.; McDonald, F. E.; Marks, T. J. *J. Am. Chem. Soc.* **1999**, *121*, 3633.
- (16) Hartung, C. G.; Breindl, C.; Tillack, A.; Beller, M. *Tetrahedron* **2000**, *56*, 5157.

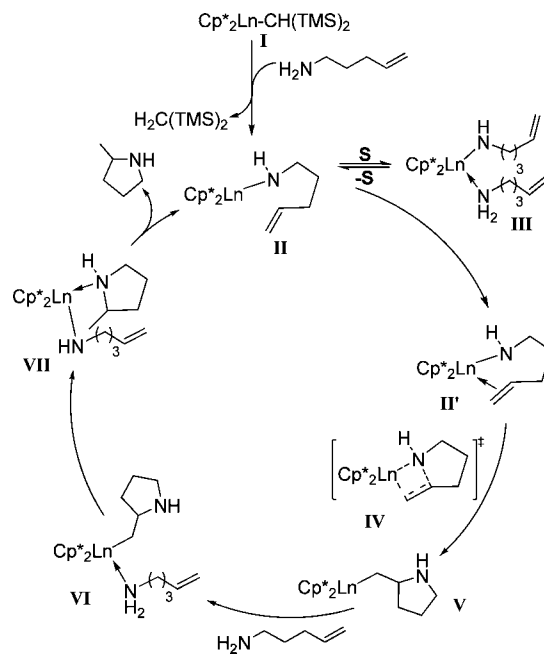
- (17) Kumar, K.; Michalik, D.; Castro, I. G.; Tillack, A.; Zapf, A.; Arlt, M.; Heinrich, T.; Böttcher, H.; Beller, M. *Chem.—Eur. J.* **2004**, *10*, 746.
- (18) Sakai, N.; Ridder, A.; Hartwig, J. F. *J. Am. Chem. Soc.* **2006**, *128*, 8134.
- (19) Zhang, W.; Werness, J. B.; Tang, W. *Org. Lett.* **2008**, *10*, 2023.
- (20) Gagné, M. R.; Marks, T. J. *J. Am. Chem. Soc.* **1989**, *111*, 4108.
- (21) Gagné, M. R.; Nolan, S. P.; Marks, T. J. *Organometallics* **1990**, *9*, 1716.
- (22) Gagné, M. R.; Brard, L.; Conticello, V. P.; Giardello, M. A.; Stern, C. L.; Marks, T. J. *Organometallics* **1992**, *11*, 2003.
- (23) Gagné, M. R.; Stern, C. L.; Marks, T. J. *J. Am. Chem. Soc.* **1992**, *114*, 275.
- (24) Tian, S.; Arredondo, V. M.; Stern, C. L.; Marks, T. J. *Organometallics* **1999**, *18*, 2568.
- (25) Hong, S.; Marks, T. J. *Acc. Chem. Res.* **2004**, *37*, 673.
- (26) Kim, Y. K.; Livinghouse, T.; Bercaw, J. E. *Tetrahedron Lett.* **2001**, *42*, 2933.
- (27) Collin, J.; Daran, J.-C.; Schulza, E.; Trifonov, A. *Chem. Commun.* **2003**, 3048.
- (28) Gribkov, D. V.; Hultsch, K. C.; Hampel, F. *Chem.—Eur. J.* **2003**, *9*, 4796.
- (29) O'Shaughnessy, P. N.; Knight, P. D.; Morton, C.; Gillespie, K. M.; Scott, P. *Chem. Commun.* **2003**, 1770.
- (30) O'Shaughnessy, P. N.; Scott, P. *Tetrahedron: Asymmetry* **2003**, *14*, 1979.
- (31) Kim, Y. K.; Livinghouse, T.; Horino, Y. *J. Am. Chem. Soc.* **2003**, *125*, 9560.
- (32) Gribkov, D. V.; Hultsch, K. C. *Chem. Commun.* **2004**, 730.
- (33) O'Shaughnessy, P. N.; Gillespie, K. M.; Knight, P. D.; Munslow, I. J.; Scott, P. *Dalton Trans.* **2004**, 2251.
- (34) Rastätter, M.; Zulus, A.; Roesky, P. W. *Chem. Commun.* **2006**, 874.

focused on group 4 complexes, with cationic zirconium catalysts^{36,37} and neutral zirconium^{38–53} and titanium^{43,48,49,54–59} systems.

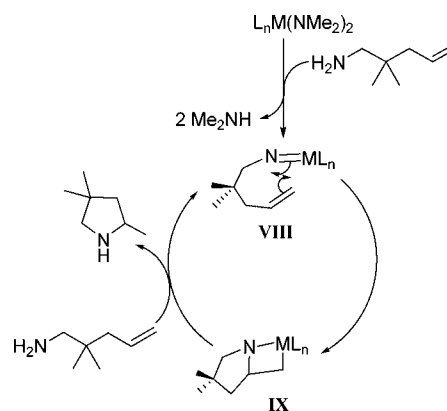
The established mechanism for lanthanide systems involves turnover-limiting C=C insertion into the Ln–N amido σ -bond.^{20,23,25} The observed rate law, $\sim[\text{Ln}]^1[\text{aminoalkene}]^0$, thermodynamic parameters, and other observations are consistent with this mechanism (Scheme 1).⁶⁰ The precatalyst **I** reacts quickly with the aminoalkene substrate to give the activated amido catalyst **II**, which is in equilibrium with the amino–amido complex **III**. The coordination isomer of **II**, i.e., **II'**, undergoes rate-limiting insertion of the coordinated alkene into the Ln–N bond via transition state **IV** to form the heterocyclic product **V**, which is protolyzed via **VI** and **VII** and releases product to regenerate **II**.

While a similar amido mechanism may be operative for the cationic zirconium species,^{36,37} recent cyclohydroamination studies using neutral group 4 complexes allow the possibility of an imido mechanism (Scheme 2) analogous to Bergman's hydroamination of alkynes/allenes.⁶¹ Nevertheless, while the [2+2] cycloadditions of group 4 imides with alkynes and allenes have been investigated using both experimental^{61–64} and computational^{65–67} methods, such a reaction of unstrained

Scheme 1. The σ -Bond Insertative Mechanism (Amido) for Cyclohydroamination



Scheme 2. Imido Mechanism for Cyclohydroamination



alkenes (e.g., at **VIII**, Scheme 2) is otherwise essentially unprecedented.^{68,69}

Schafer showed that bis(amido) complex **X** (Chart 1) and imido species **XI** had similar activity for aminoalkene cyclohydroamination, with turnover numbers of up to 12 h^{-1} at 110°C , and thus a common catalytic intermediate was proposed.⁴⁰ The inactivity for secondary amines was attributed to their inability to form imido species. It was noted, however, that a lanthanide-like amido mechanism was not excluded.

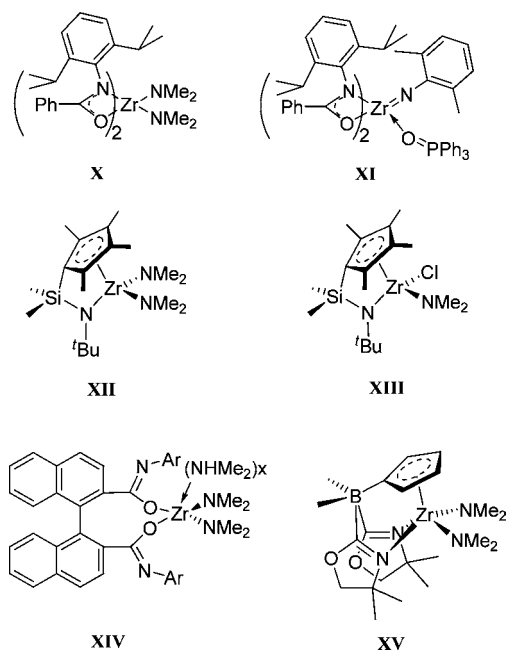
In a thorough investigation into the mechanism of actinide and Zr constrained geometry catalysts (CGCs), it was shown that, e.g., **XII** (Chart 1) was moderately active in the cyclohydroamination of a range of substrates.⁶⁰ Rates were much lower than those of the analogous Ln^{24} and An^{70} systems, and the mixed chloro–amido complex **XIII** was a significantly more active catalyst for the cyclohydroamination of both primary and

- (35) Rastätter, M.; Zulus, A.; Roesky, Peter, W. *Chem.—Eur. J.* **2007**, *13*, 3606.
 (36) Knight, P. D.; Munslow, I.; O'Shaughnessy, P. N.; Scott, P. *Chem. Commun.* **2004**, 894.
 (37) Gribkov, D. V.; Hultsch, K. C. *Angew. Chem., Int. Ed.* **2004**, *43*, 5542.
 (38) Kim, H.; Lee, P. H.; Livinghouse, T. *Chem. Commun.* **2005**, 5205.
 (39) Kim, H.; Kim, Y. K.; Shim, J. H.; Kim, M.; Han, M.; Livinghouse, T.; Lee, P. H. *Adv. Synth. Catal.* **2006**, *348*, 2609.
 (40) Thomson, R. K.; Bexrud, J. A.; Schafer, L. L. *Organometallics* **2006**, *25*, 4069.
 (41) Watson, D. A.; Chiu, M.; Bergman, R. G. *Organometallics* **2006**, *25*, 4731.
 (42) Gott, A. L.; Clarke, A. J.; Clarkson, G. J.; Scott, P. *Organometallics* **2007**, *26*, 1729.
 (43) Marcseková, C.; Loos, C.; Rominger, F.; Doye, S. *Synlett* **2007**, *16*, 2564.
 (44) Wood, M. C.; Leitch, D. C.; Yeung, C. S.; Kozak, J. A.; Schafer, L. L. *Angew. Chem., Int. Ed.* **2007**, *46*, 354.
 (45) Gott, A. L.; Clarke, A. J.; Clarkson, G. J.; Scott, P. *Chem. Commun.* **2008**, 1422.
 (46) Gott, A. L.; Clarkson, G. J.; Deeth, R. J.; Hammond, M. L.; Morton, C.; Scott, P. *Dalton Trans.* **2008**, 2983.
 (47) Li, X.; Haibin, S.; Zi, G. *Eur. J. Inorg. Chem.* **2008**, *2008*, 1135.
 (48) Majumder, S.; Odom, A. L. *Organometallics* **2008**, *27*, 1174.
 (49) Müller, C.; Saak, W.; Doye, S. *Eur. J. Org. Chem.* **2008**, *2008*, 2731.
 (50) Zi, G.; Wang, Q.; Xiang, L.; Song, H. *Dalton Trans.* **2008**, 5930.
 (51) Leitch, D. C.; Payne, P. R.; Dunbar, C. R.; Schafer, L. L. *J. Am. Chem. Soc.* **2009**, *131*, 18246.
 (52) Zi, G.; Liu, X.; Xiang, L.; Song, H. *Organometallics* **2009**, *28*, 1127.
 (53) Reznichenko, A. L.; Hultsch, K. C. *Organometallics* **2010**, *29*, 24.
 (54) Bexrud, J. A.; Beard, J. D.; Leitch, D. C.; Schafer, L. L. *Org. Lett.* **2005**, *7*, 1959.
 (55) Lee, A. V.; Schafer, L. L. *Organometallics* **2006**, *25*, 5249.
 (56) Müller, C.; Loos, C.; Schulenberg, N.; Doye, S. *Eur. J. Org. Chem.* **2006**, *2006*, 2499.
 (57) Bexrud, J. A.; Li, C.; Schafer, L. L. *Organometallics* **2007**, *26*, 6366.
 (58) Müller, C.; Koch, R.; Doye, S. *Chem.—Eur. J.* **2008**, *14*, 10430.
 (59) Lian, B.; Spaniol, T. P.; Horriño-Martínez, P.; Hultsch, K. C.; Okuda, J. *Eur. J. Inorg. Chem.* **2009**, *2009*, 429.
 (60) Stubbert, B. D.; Marks, T. J. *J. Am. Chem. Soc.* **2007**, *129*, 6149.
 (61) Walsh, P. J.; Baranger, A. M.; Bergman, R. G. *J. Am. Chem. Soc.* **1992**, *114*, 1708.
 (62) Baranger, A. M.; Walsh, P. J.; Bergman, R. G. *J. Am. Chem. Soc.* **1993**, *115*, 2753.
 (63) Sun Yeoul, L.; Bergman, R. G. *Tetrahedron* **1995**, *51*, 4255.
 (64) Pohlík, F.; Doye, S. *Angew. Chem., Int. Ed.* **2001**, *40*, 2305.
 (65) Straub, B. F.; Bergman, R. G. *Angew. Chem., Int. Ed.* **2001**, *40*, 4632.
 (66) Tobisch, S. *Dalton Trans.* **2006**, 4277.
 (67) Tobisch, S. *Chem.—Eur. J.* **2007**, *13*, 4884.

(68) Walsh, P. J.; Hollander, F. J.; Bergman, R. G. *Organometallics* **1993**, *12*, 3705.

(69) Polse, J. L.; Andersen, R. A.; Bergman, R. G. *J. Am. Chem. Soc.* **1998**, *120*, 13405.

(70) Stubbert, B. D.; Stern, C. L.; Marks, T. J. *Organometallics* **2003**, *22*, 4836.

Chart 1. Selection of Recent Zr Catalysts for Cyclohydroamination

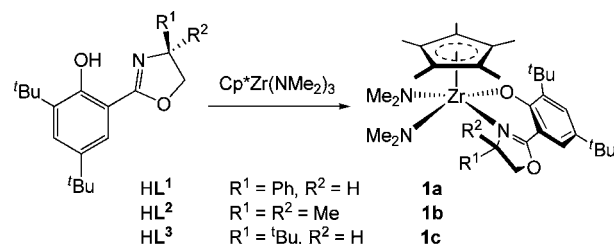
secondary aminoalkenes than the bis(amido) complex **XII**. This is particularly interesting as **XIII** cannot form an imido species, ruling out that pathway. Thermodynamic and rate law data were also consistent with an amido mechanism analogous to that followed by the Ln and An CGCs, and it was argued⁶⁰ that it was unnecessary to invoke the imido mechanism for group 4 complexes elsewhere.

More recently, the very active Zr systems **XIV**⁵³ and **XV**⁷¹ have been reported for the cyclohydroamination of a range of aminoalkene substrates, although not secondary aminoalkenes, even at elevated temperatures. Preliminary kinetic studies indicated in both cases that the catalysis was first-order in both substrate and catalyst and that substantial kinetic isotope effects were observed.

Hence, it would seem that our observation in 2008 of an unexpectedly fast and efficient enantioselective cyclohydroamination of aminoalkenes using chiral-at-metal half-sandwich diamide catalysts⁴⁵ has been followed by still faster systems. This rise of the importance of zirconium in cyclohydroamination catalysis is accompanied by a number of recent preliminary mechanistic studies which propose productive imido intermediates akin to those present in Bergman's alkyne/allene hydroamination system.^{61,62} Here we report kinetic and other mechanistic investigations into our half-sandwich system which exclude the amido insertative mechanism and are consistent with an imido/alkene cycloaddition mechanism in which, like the Bergman alkyne catalysts, the imido formation is rate-limiting.

Results and Discussion

The Zr precatalysts were obtained through the reaction of Cp*Zr(NMe₂)₃⁷² with the appropriate salicyloxazoline proligand (Scheme 3).^{45,73–75} For the detailed kinetic studies described

Scheme 3. Synthesis of Precatalysts 1

here, we chose to study in the main two readily available precatalysts: (i) S_C,S_{Zr}-[Cp***L**¹Zr(NMe₂)₂] (**1a**) contains an optically pure phenylglycinol-derived ligand and is present as a single diastereomer with respect to the stereogenic center at Zr;⁴⁵ (ii) [Cp***L**²Zr(NMe₂)₂] (**1b**) contains a more sterically demanding but achiral ligand and is formed as a racemic mixture. We have shown that chloride and alkyl complexes related to **1b** undergo slow racemization on the NMR chemical shift time scale ($\Delta G_{298}^{\ddagger} \approx 75 \text{ kJ mol}^{-1}$) and also are modestly active though stable and well-defined single-site precatalysts for olefin polymerization.⁷³

Aminopentenes **2a,b** and aminohexenes **3a,b** were chosen as test substrates in order to probe the effect of substituent bulk and ring size on the rate of cyclization (Table 1).

Kinetic Studies toward the Rate Equation. Quantitative kinetic studies of the cyclohydroamination of aminoalkene substrates were carried out using in situ ¹H NMR monitoring. Ferrocene was employed as an internal ¹H NMR integration standard, as it can be readily differentiated from the substrate, product, and catalyst resonances. The disappearance of the substrate olefinic CH signal was monitored as a function of time and normalized versus the internal standard. Cyclizations were performed with 10 mol % catalyst so that reactions could be run to completion or at least span sufficient half-lives within a reasonable time period.

Linear plots of substrate concentration versus time were obtained for runs in the range 60–90 °C, indicating that the reactions are zero-order in substrate. Figure 1 shows a typical series of runs for the cyclization of 4-pentenylamine **2a** catalyzed by **1a**.

The linear response of the observed rate of reaction versus precatalyst concentration is shown in Figure 1b. The initial substrate concentration was kept constant. In addition, the van't Hoff plot of Figure 1c has a slope of ca. 1.1, indicating that the reaction is first-order in catalyst.

The rate equation thus determined for this catalytic process is given in eq 1.

$$-d[\text{substrate}]/dt = k[\text{catalyst}]^1[\text{substrate}]^0 \quad (1)$$

Given that the precatalysts used here are strictly mononuclear, with sterically bulky ligands and high coordination number, the observation of first-order kinetics in catalyst is as expected. We note that preliminary evidence for a first-order dependence of rate on [aminoalkene] has been presented for other zirconium catalysts.^{40,49,53,71} These systems are, however, strikingly different from the present system in that they have lower coordination number and/or are sterically unencumbered. The

(71) Manna, K.; Ellern, A.; Sadow, A. D. *Chem. Commun.* **2010**, 46, 339.

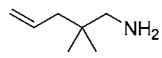
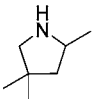
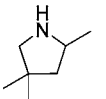
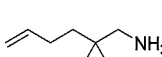
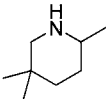
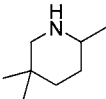
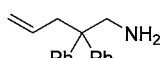
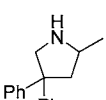
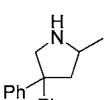
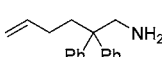
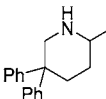
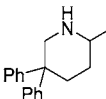
(72) Irigoyen, A. M.; Martin, A.; Mena, M.; Palacios, F.; Yélamos, C. *J. Organomet. Chem.* **1995**, 494, 255.

(73) Coles, S. R.; Clarkson, G. J.; Gott, A. L.; Munslow, I. J.; Spitzmesser, S. K.; Scott, P. *Organometallics* **2006**, 25, 6019.

(74) Westmoreland, I.; Munslow, I. J.; Clarke, A. J.; Clarkson, G.; Deeth, R. J.; Scott, P. *J. Organomet. Chem.* **2006**, 691, 2228.

(75) Gott, A. L.; Clarke, A. J.; Clarkson, G. J.; Munslow, I. J.; Wade, A. R.; Scott, P. *Organometallics* **2008**, 27, 2706.

Table 1. Effect of Varying Substrate on Kinetic and Thermodynamic Parameters for Cyclohydroamination Mediated by $[\text{Cp}^*\text{L}^1\text{Zr}(\text{NMe}_2)_2]$, **1a**, and $[\text{Cp}^*\text{L}^2\text{Zr}(\text{NMe}_2)_2]$, **1b**^a

Entry	Catalyst	Substrate	Product	N_t^b (90°C)	ΔH^\ddagger (kcalmol ⁻¹)	ΔS^\ddagger (calK ⁻¹ mol ⁻¹)	E_A (kcalmol ⁻¹)
1	1a			2.4	20.8 (0.3)	-16.1 (0.9)	21.5 (0.3)
2	1b	2a		7.9	21.2 (0.4)	-12.7 (1.2)	21.9 (0.4)
3	1a			8.7	19.5 (0.5)	-17.1 (1.4)	20.2 (0.5)
4	1b	3a		11.7	17.1 (0.1)	-22.8 (0.3)	17.7 (0.1)
5	1a			2.7	19.0 (0.4)	-20.9 (1.1)	19.7 (0.4)
6	1b	2b		48.3	17.0 (0.2)	-20.7 (0.6)	17.6 (0.2)
7	1a			2.6	18.5 (0.4)	-22.6 (1.2)	19.2 (0.4)
8	1b	3b		2.2	19.5 (0.4)	-19.8 (1.1)	20.2 (0.4)

^a 10 mol % of catalyst used, 90 °C, toluene-*d*₈. ^b N_t calculated from least-squares fit to data, over at least three half-lives. Parameters in parentheses represent 3 σ values derived from the least-squares fit.

most fruitful comparison is with Marks's lanthanide systems, for which a wealth of mechanistic information is available, and for which an imido mechanism is excluded; a comparison of these f-element data with those obtained for the current zirconium system is given in Table 2.

Thermodynamic Parameters. The kinetic data obtained at a range of temperatures (e.g., Figure 1a) were used in standard Eyring (Figure 2a) and Arrhenius (Figure 2b) analyses to obtain thermodynamic parameters for the reactions. The results are detailed in Table 1 and summarized alongside other mechanistic observations in Table 2.

The ΔH^\ddagger values for all zirconium catalyst/substrate combinations in Table 1 fall within a narrow range: ca. 17–21 kcal mol⁻¹ (eight examples). The ΔS^\ddagger value range of ca. -13 to -23 cal K⁻¹ mol⁻¹ is also remarkably uniform, given the many potential influences on this parameter. This is all consistent with a common transition-state mechanism in the catalysis.

While to our knowledge no thermodynamic parameters are available for other zirconium catalysts for this type of reaction, the ΔH^\ddagger value of 12.7(1.4) kcal mol⁻¹ for $\text{Cp}^*\text{LaCH}(\text{TMS})_2$ ²³ is substantially lower than those observed here. This implies that the bond-making/breaking events in the region of transition state are less well balanced in the case of the current system than for the lanthanides, and it is this matter that appears to be at the heart of the relative activities of the two classes of catalyst (i.e., why Zr, even in this relatively fast system, is slower than lanthanide). Even though direct comparison between the catalyst systems is not a simple matter, Hammond's postulate suggests that a more endothermic rate-determining step implies a less stable reactive intermediate for the current system than for the lanthanide catalysts.

The ΔS^\ddagger value of -27.0(4.6) cal K⁻¹ mol⁻¹ for the lanthanocene²³ indicates a highly ordered transition state; this is

consistent with the olefin insertion process of Scheme 1. In the current zirconium system, the values of -13 to -23 cal K⁻¹ mol⁻¹ indicate significantly less ordering in the transition state, and our proposed mechanism needs to take this into account.

Catalyst Steric Effects. In preliminary work, we noted that the more sterically encumbered salicyloxazoline zirconium systems appeared to be faster catalysts for cyclohydroamination.⁴⁵ The kinetic results summarized in Table 1 also demonstrate this trend, with bulkier complex **1b** giving consistently higher turnover frequency than **1a**. Examination of the accompanying thermodynamic factors would indicate, for example, that the increase in observed rate from entry 1 to 2 is accompanied by lower entropy penalty ΔS^\ddagger . The rate difference between entries 3 and 4, however, while less substantial, arises from the lower ΔH^\ddagger more than compensating for a more negative ΔS^\ddagger . For entries 5 and 6, the difference in ΔH^\ddagger clearly dominates. Whatever the detail of the origins of this phenomenon, the higher activity of the bulkier catalysts in this series is in contravention with the otherwise universal trend of faster cyclohydroamination catalysis by systems with greater metal accessibility. For example, the lanthanide cyclopentadienyl catalysts with more open coordination spheres have the higher turnover frequencies.²⁵

We have previously reported the molecular structure of **1c**,⁴⁵ and this is shown with the molecular structure of **1b** in Figure 3. The two structures were compared using the *align* algorithm in PyMol.⁷⁶ Corresponding atom pairs from each molecule are overlaid and optimized to minimize the root-mean-square deviation (rmsd) between the structures. A good fit was obtained from aligning (from the structure of **1b**) the Zr atom, the

(76) DeLano, W. L. *The PyMOL Molecular Graphics System*; DeLano Scientific: San Carlos, CA, 2002; <http://www.pymol.org>.

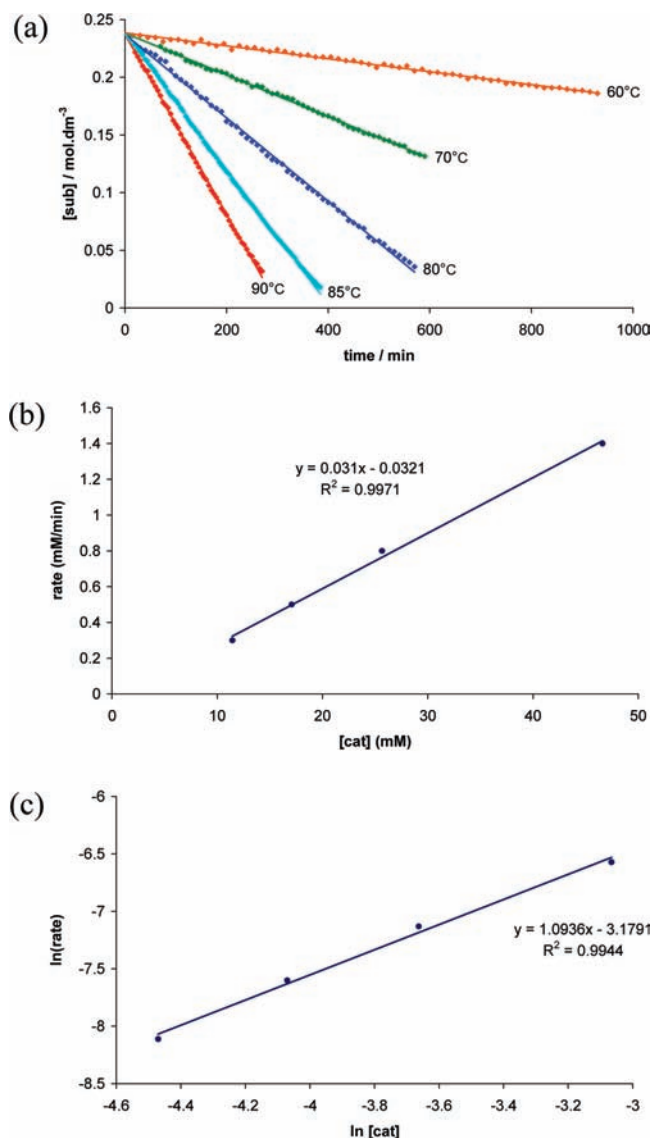


Figure 1. Kinetic plots of hydroamination/cyclization of **2a** using pre-catalyst **1a** in toluene-*d*₆: (a) zero-order plots of [substrate] versus time, 60–90 °C; (b) determination of order with respect to catalyst at 90 °C; (c) Van't Hoff plot for 90 °C data using the pre-catalyst. The lines are least-squares fits to the data points.

heteroatoms of the ligands [O(1), N(1), N(2), N(3)], the interconnecting carbon atoms of the salicyloxazoline ligand [C(1), C(6), C(7)], the geminally substituted carbon atom of the oxazoline C(9), the methyl group C(10), and the ring carbons of the Cp*, all with the corresponding atoms on **1c**. The optimized overlay of the two structures is shown in Figure 4. Qualitatively, it can be seen that, despite the dimethyl substitution at the oxazoline C(9), the inner coordination spheres of the two complexes have very similar arrangements of these moieties, and the rmsd fit was found to be 0.114 Å. Correspondingly, most of the relevant bond lengths and angles are very similar between structures. The steric demand of the additional substituent at C(9) in **1b** compared with **1a** and **1c** is, however, manifest in the orientation of the dimethylamido substituents. In **1c**, this unit is free to rotate to attain a sterically undemanding orientation [torsion angle Cp_{centroid}–Zr(1)–N(2)–C(23) ca. 50.3°], while for **1b** it is required to orient “vertically” [torsion angle Cp_{centroid}–Zr(1)–N(2)–C(21) ca. 12.5°], thus interacting

with the Cp* ligand. This is discussed further in the context of the shape of the proposed transition state for the catalytic reaction.

A number of further observations substantiate the idea that catalysts **1** are fast as a result of, rather than despite, their high coordination number and their steric bulk. For example, unlike Zr(NMe₂)₄,⁵⁴ six-coordinate Cp*Zr(NMe₂)₃⁷² and L₂Zr(NMe₂)₂⁷⁴ show respectively little and no conversion of these substrates. Chiral amidate^{42,44} and phosphinic/thiophosphinic amidate^{38,41} catalysts are sterically unsaturated but are nevertheless substantially slower than **1a–c**. The turnover frequencies observed for seven-coordinate **1b** are at least 2 orders of magnitude higher than those of the less congested, six-coordinate (Cp*SiMe₂NBu^t)Zr(NMe₂)₂ ($N_t = 0.07 \text{ h}^{-1}$ at 100 °C).⁶⁰ We note, however, that a very recent preliminary study of a zwitterionic zirconium diamido catalyst, employing a mixed cyclopentadienyl–bisoxazolonyl borato ligand, indicates substantial activity at room temperature.⁷¹

Ring Size. To our knowledge, all previously reported cyclohydroamination catalysts based on lanthanides^{20,23,77–79} cyclize five-membered (pyrrolidine) rings at significantly higher rates than six-membered (piperidine) rings. This is unsurprising for processes in which the cyclization is the rate-determining step. For systems based on group 4 metals, the general trend is the same.^{38,40,53,54,56,80}

In Table 1, comparison of the turnover frequencies for entries 1 and 3 shows that, in the case of the *gem*-dimethyl substrates **2a** and **3a**, the six-membered ring ($N_t = 8.7 \text{ h}^{-1}$) is cyclized noticeably faster than the five-membered ring (2.4 h⁻¹) using catalyst **1a**. For the faster, bulkier catalyst **1b**, the trend is still evident although less pronounced (entries 2 and 4). Hence, cyclization cannot be rate-determining for these catalytic systems. Catalyst **1a** is capable of cyclizing 2,2-dimethyl-6-heptenylamine, albeit very slowly ($N_t = 0.05 \text{ h}^{-1}$); however, no reactivity toward this substrate was observed with catalyst **1b**. This implies that ring-closure may be rate-determining for larger rings and that the increased steric bulk of **1b** disfavors this cyclization.

Interestingly also, comparison of entries 1 and 5 shows that there is little effect on the performance of catalyst **1a** upon increasing the size of the *gem*-dialkyl group from methyl to phenyl. At the same time, the bulkier catalyst **1b** (entries 2 and 6) shows a dramatic increase in N_t , from 7.9 to 48.3 h⁻¹, on moving to the bulkier substrate.

Effect of Added Bases. Lewis acidic catalysts for cyclohydroamination, such as lanthanide²³ and rare-earth metal systems,^{32,81} are strongly affected by the presence of non-protic bases such as THF. For the lanthanocenes, using THF as the reaction solvent decreases the rate and causes a departure from the standard rate law; THF competes very effectively for coordination sites at the metal. The yttrium systems are sensitive to even a few equivalents of THF, with turnover numbers decreasing by almost 50% after addition of 5 equiv.⁸¹

Remarkably, the cyclohydroamination reactions of substrates **2a** and **3a** using catalysts **1a** and **1b** conducted in neat THF

(77) Giardello, M. A.; Conticello, V. P.; Brard, L.; Gagne, M. R.; Marks, T. J. *J. Am. Chem. Soc.* **1994**, *116*, 10241.

(78) Hong, S.; Tian, S.; Metz, M. V.; Marks, T. J. *J. Am. Chem. Soc.* **2003**, *125*, 14768.

(79) Gribkov, D. V.; Hultsch, K. C.; Hampel, F. *J. Am. Chem. Soc.* **2006**, *128*, 3748.

(80) Bexrud, J. A.; Schafer, L. L. *Dalton Trans.* **2010**, 39, 361.

(81) Hultsch, K. C.; Hampel, F.; Wagner, T. *Organometallics* **2004**, *23*, 2601.

Table 2. Comparison of Mechanistic Data for Lanthanocene Catalysts and the Current Zr System

observation	Cp ₂ LnX	Cp [*] LZr(NMe ₂) ₂	conclusion
-d[substrate]/dt ∝ added THF	[Ln] ¹ [substrate] ⁰	[Zr] ¹ [substrate] ⁰	substrate not lost or gained before rate-determining TS of either catalyst Zr not acting as Lewis acid in RDS
added non-cyclizable amine	inhibits	inhibits	substrate activated as amido unit is involved in both RDSs
rate dependence on ring size	5 ≫ 6	5 ~ 6	Cyclization is RDS for Ln but not for Zr
KIE (k _H /k _D)	2.7–5.2	2.5–3.0	both have N–H bond breaking in RDS
ΔS [‡] (cal/K·mol)	-27(2)	-13 to -23	highly ordered TS for Ln, less ordered for Zr
ΔH [‡] (kcal/mol)	13(5)	17–21	bond-breaking/making less in balance for Zr
ligand steric bulk	reduces rate	increases rate	progression to TS involves increased crowding for Ln but reduced crowding for Zr
secondary aminoalkenes?	yes (slower)	no	implies imido for Zr
valencies required at M	1	2	excludes amido for Zr

proceeded at rates which were indistinguishable from those of the same reactions conducted in the more conventional toluene solvent. A comparison of two such reactions is shown in Figure 5. Unlike previous systems, the rate-limiting step for these catalyses does not involve the metal acting as a Lewis acid in the rate-determining step. There are no free coordination sites in the four-legged piano stool structure at which THF might be expected to bind strongly. Also, we know that the six-coordinate cationic center in [Cp^{*}LZrMe]⁺[BAR^F₄]⁻ does not readily coordinate ethylene (vide infra).⁷³

Marks has shown that the addition of a non-cyclizable amine such as *n*-propylamine to cyclohydroamination reactions catalyzed by lanthanocenes significantly decreases the rate of the reaction²³ and has interpreted this behavior on the basis of competition between the cyclizable and non-cyclizable amines for binding to the metal as amido units. In the present zirconium system, the behavior was qualitatively similar. Figure 6a shows how the rate of substrate consumption is affected by increasing concentration of *n*-hexylamine. As can be seen in the plots of ln[substrate] versus time in Figure 6b, the order of reaction

appears to move from zero- toward first-order in substrate with increasing concentration of hexylamine.

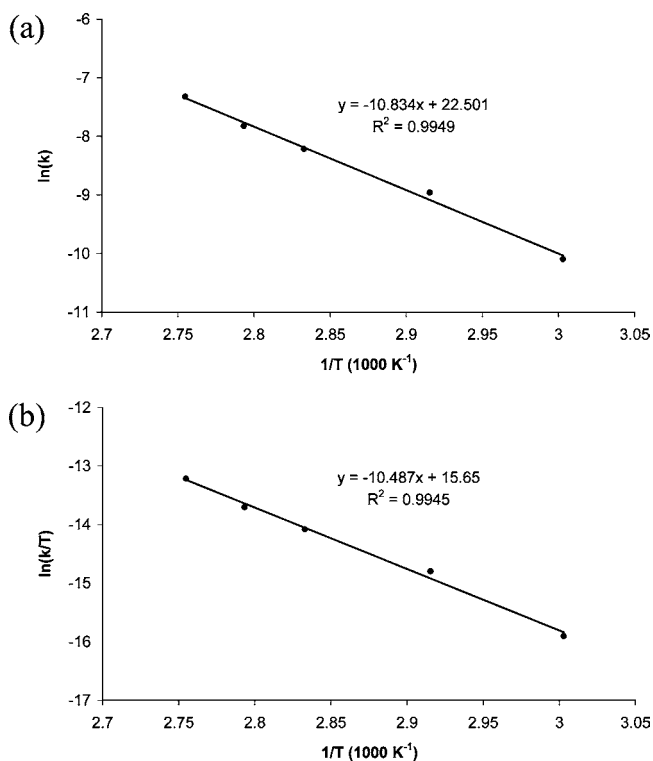


Figure 2. Cyclohydroamination of **2a** using precatalyst **1a** in toluene-*d*₈: (a) Eyring plot and (b) Arrhenius plot. The lines are least-squares fits to the data points.

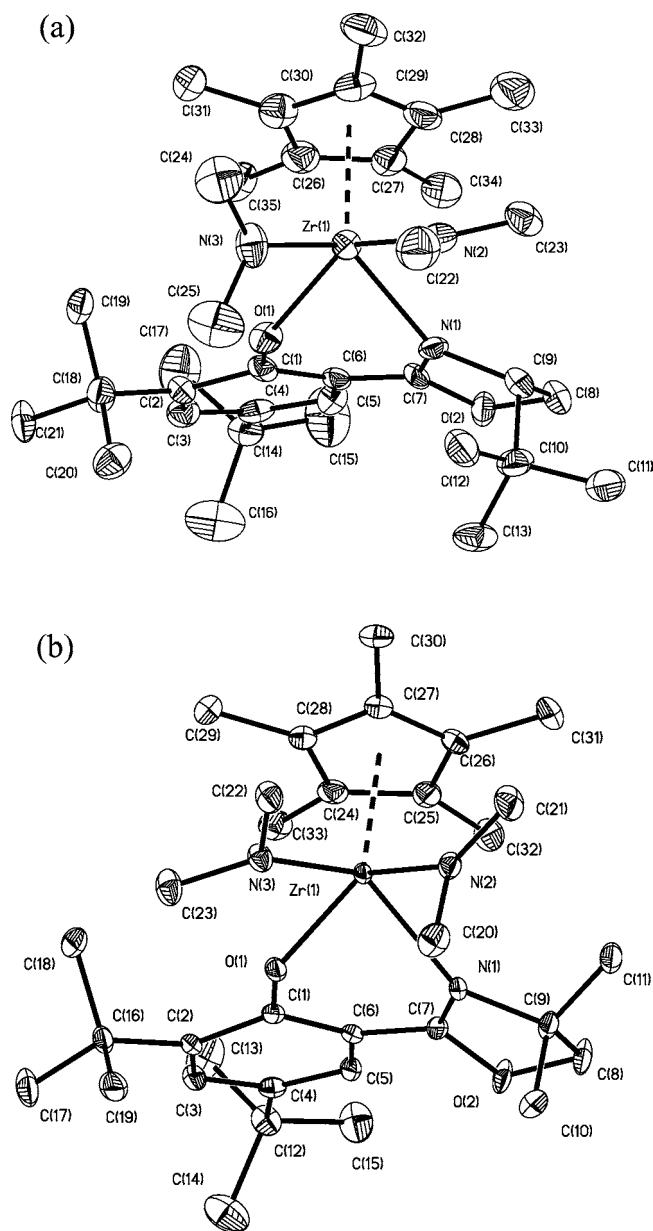


Figure 3. Molecular structures of (a) **1c** and (b) **1b**. Hydrogen atoms have been removed for clarity. Thermal parameters are drawn at 50% probability. For both structures, only one of the very similar crystallographically independent molecules is shown. For **1b**, the two independent molecules are diastereomeric.

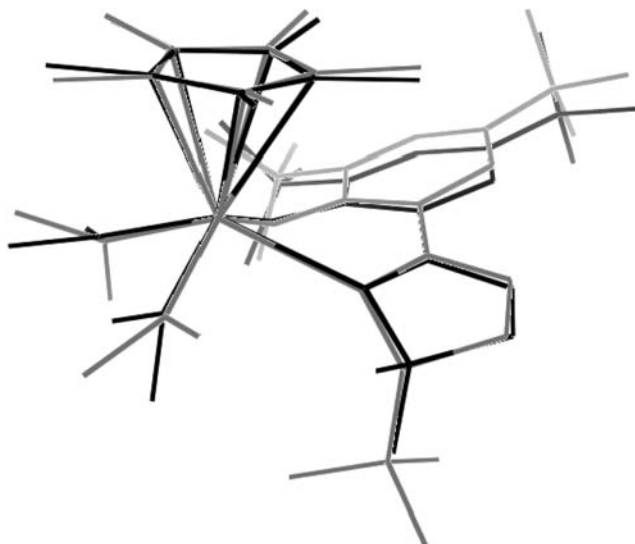


Figure 4. Overlay plot of the molecular structure of **1c** (gray) with the appropriate diastereomer of **1b** (black).

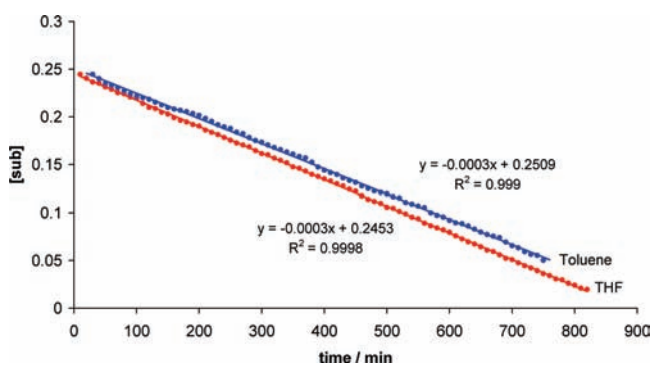


Figure 5. Kinetic plots of [substrate] versus time for cyclohydroamination of **3a** at 60 °C, using precatalyst **1a** in toluene-*d*₈ (blue) and THF-*d*₈ (red). [cat.]₀ = 0.025 M. The lines are least-squares fits to the data points.

Kinetic Isotope Effect. Measurement of the rate of cyclization of *N*-deuterated **2a** with **1a** led to $N_t = 0.78 \text{ h}^{-1}$ and thus a KIE $k_H/k_D = 3.0$ at 90 °C. For **1b**, the turnover number was decreased to 3.2 h^{-1} , giving $k_H/k_D = 2.5$ at 90 °C. This result suggests that the rate-determining step in this catalytic process involves N–H bond-breaking.

Valencies Required at Nitrogen and Metal. We have previously noted that all catalysts **1** are inactive for the cyclohydroamination of secondary amine substrates. This contrasts with the behavior of the related constrained geometry catalysts (CGCs) $(\text{Cp}^*\text{SiMe}_2\text{NBu}')\text{ZrX}_2$,⁶⁰ which have lower coordination numbers and are rather less sterically encumbered than **1**. Secondary amine substrates cannot be cyclohydroaminated via an imido mechanism, since only one N atom valency is available. It does not follow, however, that the absence of catalytic activity for secondary amines excludes the possibility of an amido mechanism or indeed proves an imido mechanism. Secondary amine substrates are commonly cyclized at substantially lower rates than the corresponding primary amines, and given the general sluggish nature of almost all preceding zirconium-based systems, any lack of activity for secondary amines might simply arise from a negligible rate of decomposition of the catalyst under the forcing conditions required.

The mechanism of operation of the aforementioned CGC compounds is investigated in some detail by Marks,⁶⁰ who

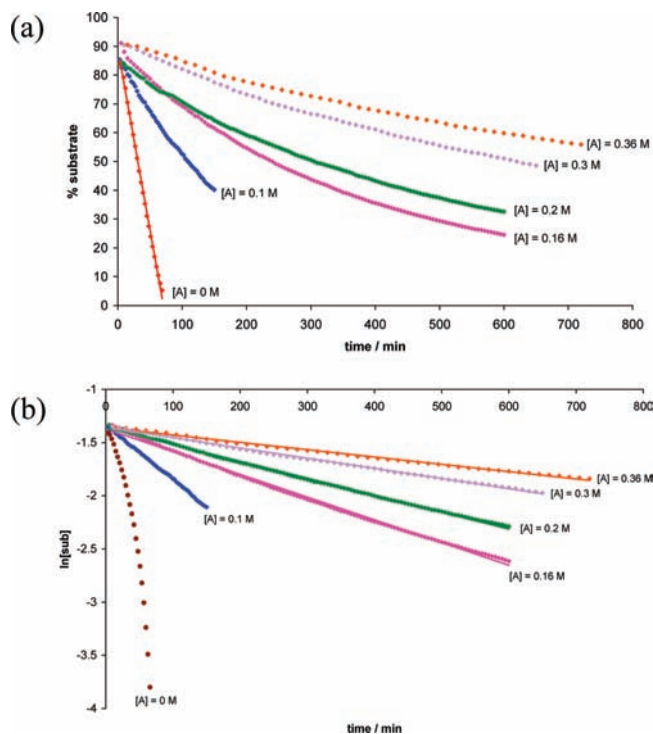


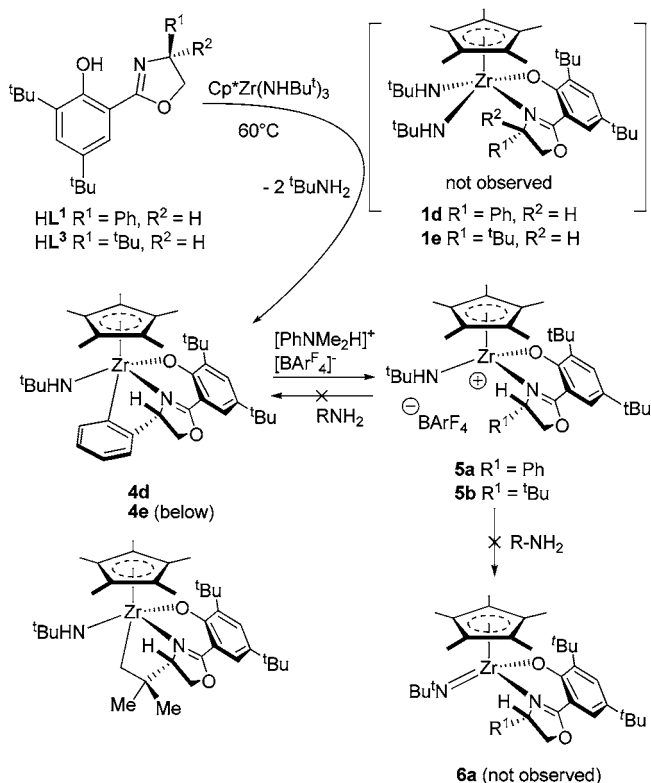
Figure 6. (a) Kinetic plots of [substrate] versus time for cyclohydroamination of **3a** using precatalyst **1a** in toluene-*d*₈ at 90 °C as a function of concentration of added *n*-hexylamine (A). (b) First-order plots of the same data. [cat.] = 0.025 M in all cases. The lines are least-squares fits to the data points.

showed that $(\text{Cp}^*\text{SiMe}_2\text{NBu}')\text{Zr}(\text{NMe}_2)\text{Cl}$, with its single readily aminolyzable amido site (single available valency), was a competent cyclohydroamination catalyst ($N_t = 0.14 \text{ h}^{-1}$) and was in fact significantly faster than $(\text{Cp}^*\text{SiMe}_2\text{NBu}')\text{Zr}(\text{NMe}_2)_2$ ($N_t = 0.07 \text{ h}^{-1}$) for steric reasons. This excludes the imido mechanism in that system, and it is concluded that a conventional (lanthanide-like) amido process is in play.

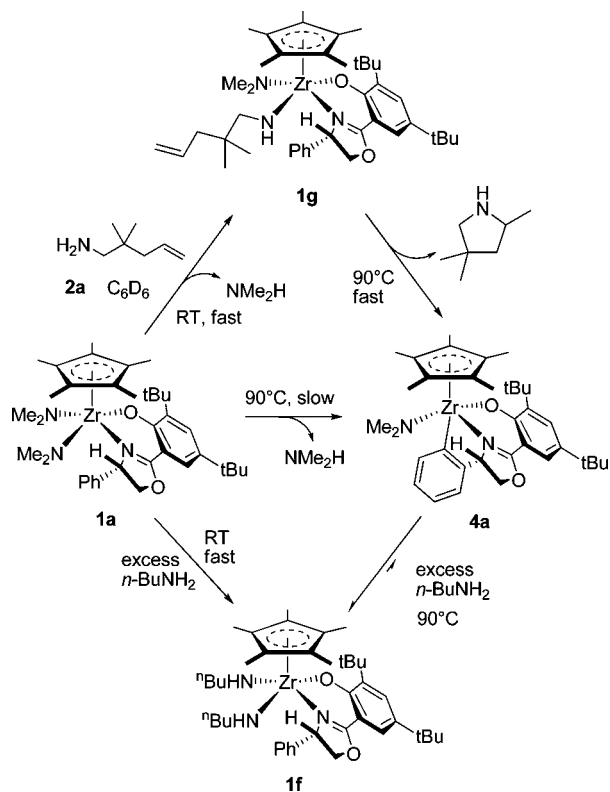
By reaction of $\text{Cp}^*\text{L}^1\text{ZrCl}_2$ with LiNMe_2 , we synthesized the system $[\text{Cp}^*\text{L}^1\text{Zr}(\text{NMe}_2)\text{Cl}]$ as a 2.3:1 diastereomeric mixture, the isomers differing only in the site substituted by NMe_2 . This isomeric mixture was completely inactive as a catalyst for cyclohydroamination of **2a**. In a control experiment, a standard catalytic run using **1a** doped with 1 molar equiv of $[\text{Cp}^*\text{L}^1\text{Zr}(\text{NMe}_2)\text{Cl}]$ cyclized **2a** with $N_t = 2.20 \text{ h}^{-1}$, slightly lower than that recorded in Table 1 (entry 1). Hence, assuming that $[\text{Cp}^*\text{L}^1\text{Zr}(\text{NMe}_2)\text{Cl}]$ does not decompose to some unknown catalytically active species, it appears that two readily aminolyzable sites are required at the metal center in the current system. This is not consistent with the operation of an amido process.

Probing Catalyst Activation and Deactivation. The triamido compound $\text{Cp}^*\text{Zr}(\text{NHBu}')_3$ ⁸² does not react with salicyloxazolines **HL**^{*n*} (*n* = 1, 3) at ambient temperature, but over 3 d at 60 °C the metalated species **4** (Scheme 4) were produced cleanly and could be isolated by sublimation. The presumed intermediate diamides **1d** and **1e** were not observed by NMR spectroscopy at this temperature. Since species like **4** are implicated in the catalysis under study here, we investigated their formation under catalytically relevant conditions.

(82) Bai, Y.; Roesky, H. W.; Noltemeyer, M.; Witt, M. *Chem. Ber.* **1992**, *125*, 825.

Scheme 4. Synthesis of Metalated **4d,e** and Amido Cations **5a,b**

Scheme 5. Stoichiometric Reactions To Probe Activation and Deactivation Pathways



Heating pure **1a** in toluene-*d*₈ at 90 °C for 24 h gave clean conversion to a metalated species **4a** (similar to **4d,e**) with loss of HNMe₂ (Scheme 5). This reaction could also be performed on a preparative scale, with essentially quantitative conversion.

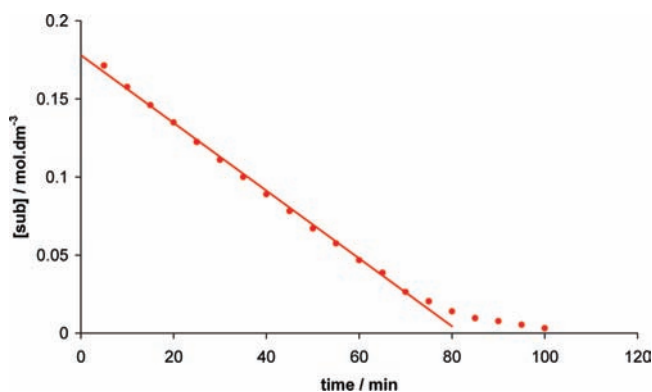


Figure 7. Kinetic plot of [substrate] versus time for cyclohydroamination of **3a** using precatalyst **1a** in toluene-*d*₈ at 90 °C. The line is a least-squares fit to the data points (up to *t* = 75 min).

This complex, like **4d,e**, has characteristic ¹H NMR resonances in the aromatic region (δ 6.52, 7.01, 7.11, and 7.32 ppm), quite separate from other peaks, thus allowing us to detect readily the presence of this and similar metalated species. In another NMR tube reaction, precatalyst **1a** was treated with excess (10 equivalents) *n*-BuNH₂ at ambient temperature, rapidly producing a species for which NMR spectra are consistent with the bis(butylamido) structure **1f**. Two equivalents of Me₂NH was released, and the new zirconium amide NH protons were observed at δ 3.47 and 4.71 ppm. Heating this sample to 90 °C for 6 h led to some broadening, but crucially no characteristic resonances for a metalated species like **4a** were observed. Hence, while the diamido precatalyst undergoes transamination rapidly, it does not convert to a metalated species in the presence of excess amine.

Precatalyst **1a** was treated with 1 equiv of aminoalkene **2a** at room temperature to give the transamination product **1g** (two diastereomers in ca. 9:1 ratio, see Supporting Information) and dimethylamine (Scheme 5). Heating the sample to 90 °C resulted in the rapid formation of cyclized product 2,4,4-trimethylpyrrolidine and metalated **4a**.

We attempted to detect the presence of orthometalated species during a cyclohydroamination run using catalyst **1a** and aminoalkene **3a** in toluene-*d*₈ using a 600 MHz NMR spectrometer. As before, the observed strictly linear plot of [substrate] vs time (Figure 7) for the first four half-lives of the reaction indicates the presence of a single kinetically important catalytic species whose concentration is not varying significantly with time. No metalated species were detected until *t* = 75 min (90% conversion), when characteristic resonances were detected at δ 6.52 ppm (Figure 8). The appearance of metalated species is accompanied by a reduction in the observed rate (Figure 7). Overall, this behavior during a catalytic run corresponds with that observed in the stoichiometric and model reactions described above in that the metalated species is not formed to a significant degree until the concentration of primary amine is low. Rate reductions at low substrate concentrations are observed with Ln and An complexes, but this has been attributed to product inhibition.^{60,83}

A catalytic reaction was conducted using 10 equiv of D₂NCH₂CMe₂CH₂CH=CH₂ (*d*₂-**2a**) and **1a**. Analysis of the NMR spectrum of the final metalated product showed that partial deuteration of the phenyl ring had occurred (Scheme 6). Resonances at δ 7.15 ppm in the ²H NMR spectrum and δ 138.4

(83) Stubbert, B. D.; Marks, T. J. *J. Am. Chem. Soc.* **2007**, *129*, 4253.

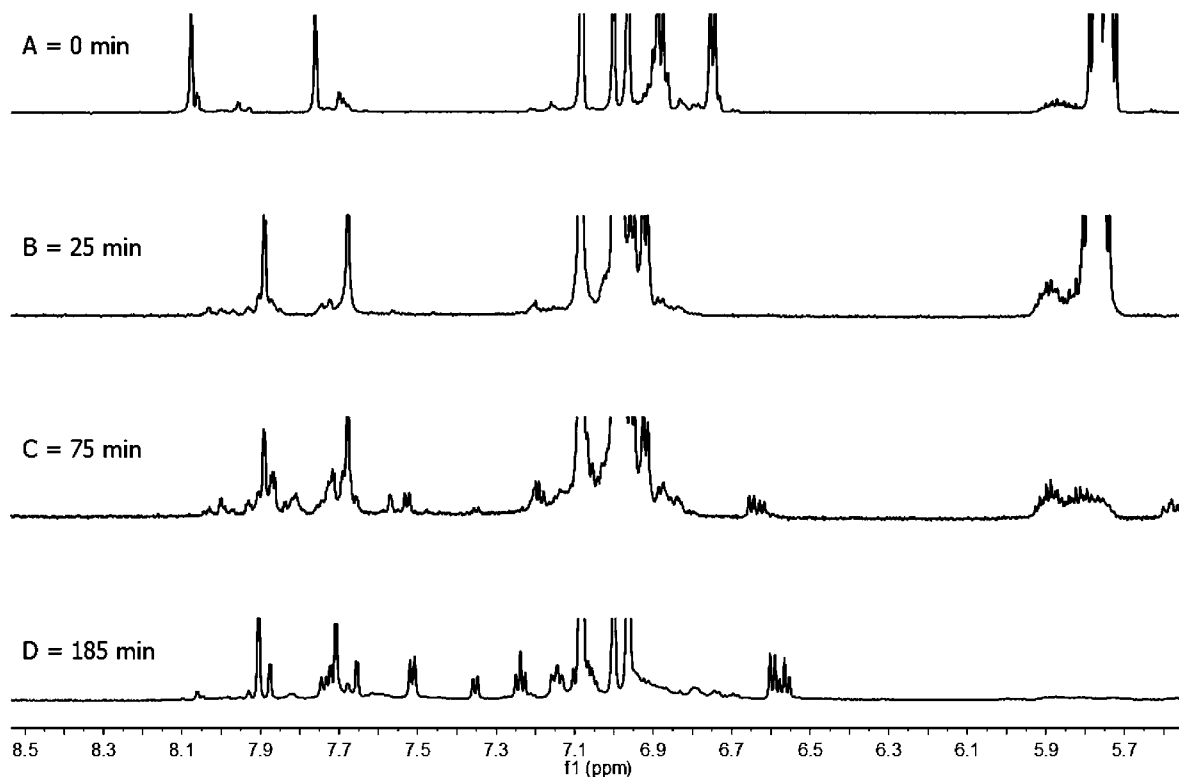
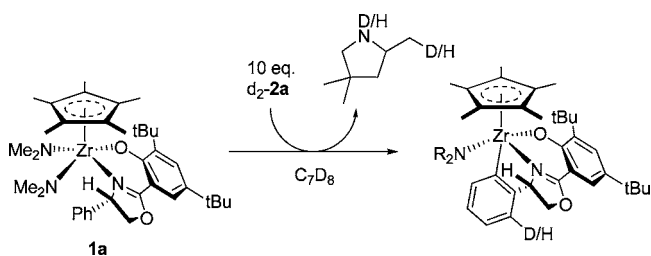


Figure 8. (A) Initial ^1H NMR spectrum (δ 6.5–8.5 ppm) of **1a** and substrate **3a** in toluene- d_6 at ambient temperature. Minor resonances correspond to the activated catalyst, where one or both NMe_2 groups have been replaced by substrate. (B) $t = 25$ min, showing activated catalyst but no CH-activated species. (C) $t = 75$ min, showing activated catalyst and a small amount of CH-activated species at a low [substrate]. (D) $t = 185$ min, showing several CH-activated species but no coordinated or free substrate.

Scheme 6. Partial Deuteration of Catalyst during Reaction with N -Deuterated Substrate

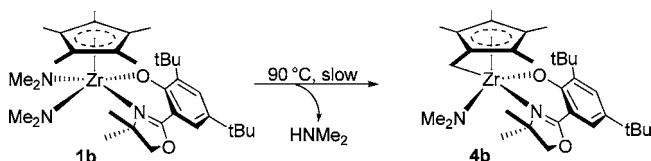


(t , $^1J_{\text{CD}} = 21$ Hz) ppm in the ^{13}C NMR correspond to the deuterated ligand, while the non-deuterated species was also evident in the ^{13}C NMR spectrum. This indicates that amido species **1** are in equilibrium with the metalated compounds at 90°C .

Precatalyst **1b** reacts with primary amines in a similar manner to **1a** (Scheme 5), forming the transaminated products with $n\text{BuNH}_2$ and **2a**. However, **1b** does not undergo metalation through CH-activation of the salicyloxazoline ligand. Prolonged heating (48 h at 90°C) of **1b** in benzene- d_6 resulted in the slow and incomplete formation of a “tuck-in” complex, **4b** (Scheme 7), as evidenced by the loss of the Cp^* protons at δ 1.81 ppm and the formation of four new methyl groups (δ 1.83, 1.90, 2.04, and 2.09 ppm). HNMe_2 was produced, and the metalated CH_2 group was observed as two doublets at δ 3.22 and 3.55 ppm ($^2J_{\text{HH}} = 13$ Hz). There is no spectroscopic evidence for the formation of **4b** during catalysis.

Cationic Systems. The first enantioselective catalysts for cyclohydroamination based on group 4 metals were alkyl cations with a weakly coordinating anion,³⁶ i.e., analogous to the many

Scheme 7. Formation of “Tuck-In” Complex **4b**



catalysts for homogeneous Ziegler–Natta polymerization of olefins by a migratory insertion mechanism.⁸⁴ These catalysts are nevertheless unusual in that they are active only for secondary amines, and thus an imido mechanism is excluded.³⁶ We were thus interested to look at the behavior of cationic derivatives of precatalysts **1**.

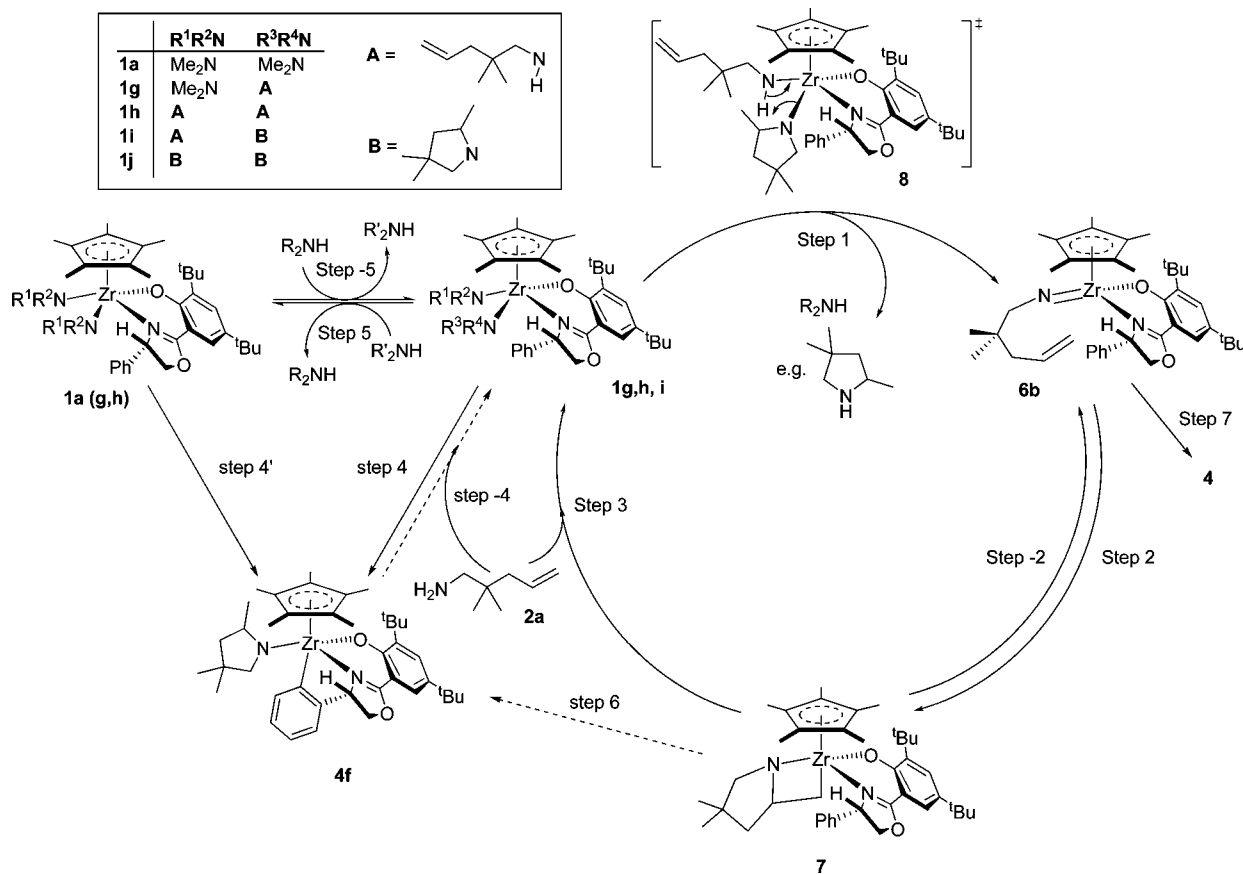
We have previously reported complexes $[\text{Cp}^*\text{ZrLMe}]^+[\text{BAR}^{\text{F}}_4]^-$ to be stable single-site catalysts for ethene polymerization. Calculations indicate that the modest catalytic activity results from the reluctance of this six-coordinate species to bind the olefin to form a four-legged piano stool.⁷³ Correspondingly, we have found that treatment of this cationic compound with aminoalkene **2a** leads to no detectable turnover of cyclohydroamination at 90°C .

Treatment of metalated species **4d** and **4e** with $[\text{PhNMe}_2\text{H}][\text{B}(\text{C}_6\text{F}_5)_4]$ yielded the complexes **5a** and **5b**, respectively, via protonolysis of the metallacyclic alkyl (Scheme 4). No evidence was found for the binding of the co-product PhNMe_2 or added THF to the metal center. These rare⁸⁵ examples of cationic amides are quite thermally stable (toluene, 90°C).⁸² Despite

(84) Chen, E. Y.-X.; Marks, T. J. *Chem. Rev.* **2000**, *100*, 1391.

(85) Kissounko, D. A.; Epshteyn, A.; Fettinger, J. C.; Sita, L. R. *Organometallics* **2006**, *25*, 1076.

Scheme 8. Catalytic Cycle for Cyclohydroamination by Catalysts 1



their coordination number being lower than those of the neutral starting materials, **5a** and **5b** are not catalysts for cyclohydroamination of primary aminoalkene **2a** or secondary aminoalkenes. For secondary amines, the lack of σ -insertion catalysis (amido mechanism) could be ascribed to the absence of an accessible coordination site. For primary amine substrates, which may react via an imido mechanism, the reasons are less obvious; retardation of catalysis by adduct formation is highly unlikely (*vide supra*). We have observed, however, that cation **5a** is stable with respect to reaction with excess amine **2a** under catalytic conditions; i.e., it is not deprotonated by amine base at the secondary amide to give $[\text{Cp}^*\text{LZr}=\text{NR}]$ or indeed to give metalated **4a**. This accords with our expectations in that the $\text{p}K_{\text{a}}$ of the NH proton in cationic zirconium primary amido species **5a** is expected to be high. The lack of catalysis is thus most probably due to the inaccessibility of the imido species from **5** under these conditions.

Catalytic Cycle. A mechanism for cyclohydroamination by precatalysts **1a** and **1b** consistent with all the observations detailed above is given in Scheme 8. In addition to the main productive cycle **1–6–7–1**, we have depicted the amide metathesis process for catalyst activation, e.g., **1a–1g**, and the catalyst deactivation processes to give (principally) **4f**.

On the basis of the kinetics and NMR experiments discussed above, we will identify the catalyst resting state and the rate-determining step, and the changes to the nature of these two elements of the mechanism, as the reaction proceeds.

Resting state: The stability of the bis-dimethylamido complex **1a** suggests that other similar bis-amido complexes may also be relatively stable compared to, say, the imido complex **6b**, the metalated species **4**, and the metallacycle **7**, providing that

any equilibrium is not significantly disturbed by the removal (by reaction or heating) of amido ligand as amine from the system. Indeed, it is clear that bis(amides) **1** are converted to metalated species **4** on heating in the absence of excess amine (steps 4, 4'). The NMR experiments above also show that bis(dimethylamido) complex **1a** reacts with pentenylamine **2a** to exchange amido ligands (step 5) rapidly at ambient temperature and at a rate that is substantially faster than the cyclization reaction (steps 1–3). Overall, these observations suggest that the resting state of the catalytic cycle at the start of the reaction, when there is excess **2a**, is the pentenylamido complex **1g** (which we have detected above) or **1h**.

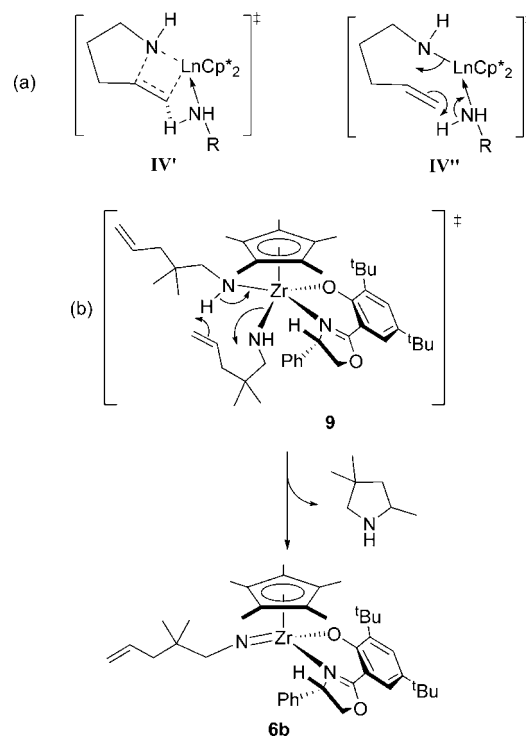
Rate-determining step: The kinetic experiments indicate that initially the reaction is first-order in catalyst and zero-order in pentenylamine starting material. Given our proposal that the mechanism of the reaction occurs via reactive imido intermediate **6b**, the rate-determining step could be the loss of an amine from the resting state to generate the imido complex (step 1). If step 1 is reversible and the reaction of this imido complex to give the metallacycle **7** by a [2+2] addition (step 2) is rate-determining, then the reaction would be inverse-order in starting material. If the reaction of this latter complex **7** with pentenylamine **2a** to regenerate the resting state (step 3) is rate-determining and the previous two steps are reversible, then, again, the reaction would be zero-order in starting material. Therefore, step 1 or 3 is rate-determining. The presence of a significant, probably primary, kinetic isotope effect on replacement of NH_2 with ND_2 in **2a** indicates that proton transfer to and from the nitrogen atoms is rate-determining. Again, this eliminates step 2 as rate-determining, as it does not involve proton transfer. If step 3 is rate-determining, with bis-amido

complex **1** of some kind as the resting state, then steps 1 and 2 must be reversible. Bergman et al. have shown that primary amines react with imido complexes quickly to give bis-amido complexes, and that related [2+2] addition reactions can be reversible.⁶¹ In our case, however, the reaction of pentenylamine starting material with metallacycle **7** may occur via a fast σ -metathesis/proton-transfer mechanism similar to that suggested in the fast exchange of amido ligands discussed above. Such a reaction of metallacycle **7** with the primary amine would involve the formation of a relatively unstrained bis-amido complex **1** from a strained amido-alkyl complex **7** and is therefore expected to be, if anything, faster than step 5. A high rate of forward reaction of metallacycle **7** with amine would render the [2+2] reaction irreversible under normal reaction conditions, and as step 2 cannot be rate-determining, step 1 must be the rate-determining step for the reaction.⁸⁶

At the end of the reaction, when the concentration of primary amine starting material is low, the rate of step 3 may, however, fall until it becomes rate-determining. In this case the reaction would continue to be zero-order in starting material as long as both steps 1 and 2 are reversible. The fall in rate in step 3 would, however, be met by a possible fall in the reverse rate of step 1. Therefore, the rate of back-reaction of imido complex **6b** and the rate of forward reaction of metallacycle **7** would fall, and a buildup in concentration of these two reactive intermediates would occur if no other reaction path was available. The NMR spectra indicate, however, that at the end of the reaction the metalated species **4** are formed. This may occur from a bis-amido complex **1** (step 4/4'), imido complex **6** (step 7), or metallacycle **7** (step 6). Metalated compounds such as **4a** are, however, poor catalysts for the cyclohydroamination reaction. The observed lowering of the reaction rate at the end the reaction is therefore caused by a reduction in the concentration of bis-amido complexes **1**.

Nature of the Rate-Determining Transition State. In Scheme 8 we depict a rate-limiting transition state **8** (step 1) in which one amido unit deprotonates the NH group of a pentenylamido unit to give the imido species **6b**. The approach to this α -elimination transition state requires some ordering of the two amido ligands. Our comparisons of the molecular structures of **1b** and **1c** above indicate that steric compression in the former would tend to reduce the amido N–Zr–N angle and facilitate bridging of an H (or D) atom between the two N atoms. We consider this to be consistent with (Table 2) the energy of this transition state not being significantly affected by the presence of THF, the observed k_H/k_D KIE, the magnitude of the negative ΔS^\ddagger values, the relatively high ΔH^\ddagger values, and the promotion of the reaction rate by steric crowding in the catalyst. We note, however, that the presence of a similar KIE in lanthanide-based cyclohydroamination led Marks some time ago to suggest an amine-assisted σ -insertative mechanism via a transition state **IV'** (Chart 2a, cf. **IV**, Scheme 1) that involves a Ln–C bond.²³ An isomeric (non-insertative) transition state **IV''** leading to concerted cyclization and protonolysis is also shown. In the present system, a similar transition state **9** is appealing since it leads to formation of cyclized product directly. Nevertheless, we can exclude the productive operation of this transition state here on the basis that (i) the bicyclic structure is highly ordered—more so than that in Marks' σ -insertative mechanism

Chart 2. Transition States for Cyclization of Amidoalkenyl Units: (a) Amine-Assisted Insertative Transition State Suggested by Marks, **IV'**, and a Similar Non-insertative Process, **IV''**, and (b) Similar Six-Membered Cyclic Transition State Applied to the Current Zr System



via transition state **IV** (Scheme 1)—and thus inconsistent with our values of ΔS^\ddagger ; (ii) the increased crowding in the active site would lead to lower activity for more crowded systems, contrary to our observations; and (iii) it involves rate-limiting ring closure and would thus be expected to lead to a significant difference between five- and six-membered cyclizations.

Conclusion

Given the sluggish nature of all but the most recent Zr-based catalysts for aminoalkene cyclohydroamination, the rate of catalysis by complexes **1** is exceptionally high. This circumstance has allowed us to perform a large number of kinetic experiments, leading to the establishment of a rate law (eq 1) which is the same as that for the original lanthanocene system, for which we find a direct comparison very helpful (Table 2). While the lanthanocenes are slowed by the presence of exogenous THF, which coordinated competitively with tethered olefin (Scheme 1), catalysts **1** are completely unaffected. This observation accords with the lack of free coordination sites at the metal in precatalysts **1**. Nevertheless, the presence of diluting non-cyclizable primary amine slows both catalysts in a qualitatively similar manner by reducing the concentration of active species containing at least one amidoalkene ligand. Another striking difference between the lanthanocenes and **1** is the independence of catalytic rate on the ring size being formed and thus the positioning of the ring-closure after the RDS. Nevertheless, both classes of catalyst display a significant KIE (k_H/k_D) in the presence of $-ND_2$ aminoalkenes, thus indicating the importance of this bond in the RDS.

Eight sets of thermodynamic parameters were determined for combinations of catalysts **1** and substrates **2** and **3**. These paint

(86) Two alternative modifications of this mechanism may be in force: (i) steps 1 and 2 are concerted and rate-determining, with step 3 fast, or (ii) step 1 is rate-determining and steps 2 and 3 are concerted. We will consider this in future computational work.

a consistent picture of a transition state which is less ordered than that for the lanthanides and in which bond-breaking outbalances bond-making to the extent that the catalytic rate for lanthanocenes is substantially higher, even for this relatively fast Zr system. Also in contrast with the lanthanocenes, rates are in order of increasing steric bulk of catalyst, e.g., **1a** < **1c** < **1b**. This is consistent with a system in which the rate-determining transition state is approached by compression of coordinated groups, and this is supported by a comparison of the molecular structures of **1b** and **1c**.

While the lanthanocenes have good activity for cyclohydroamination with secondary amines, the catalysts **1** are unable to perform this type of ring-closure. While this observation is consistent with the need for two available valencies at the N atom, it is inconclusive because the rates may simply be low rather than zero. Nevertheless, an amido mechanism is excluded by the requirement for two available valencies at the Zr center; neither diastereomers [Cp**L*Zr(NMe₂)Cl] nor cations **5a** and **5b** are catalysts. In contrast, the slower (CGC)Zr catalysts which operate by the Marks amido insertive mechanism require only one aminolyzable site.⁶⁰

A catalytic cycle is thus proposed which involves rate-determining formation of an unobserved imido species. A number of stoichiometric experiments have been conducted whose rates and products are consistent with the proposed mechanism. Specifically, metalated species **4** are observed only at the end of the reaction, when the concentration of primary amine is low.

A rate-determining transition state, consistent with all the above observations including kinetic and thermodynamic measurements, is proposed in which one amino group deprotonates its neighbor, i.e., an α -elimination analogous to that proposed in Bergman's study of zirconocene-catalyzed alkyne/allene hydroamination. A key difference is the ability of catalysts **1** to react with alkenes. The origins of this behavior will be investigated by computational means and will be reported in due course.

Unusually, the RDS (Scheme 8, step 1) and selectivity-determining step (step 2) in this reaction are different, and this has implications for future catalyst design. In particular, the relatively modest enantioselectivities we have observed (50–60%)⁴⁵ could be improved by the use of very bulky groups in place of *tert*-butyl at the salicyl unit since this will regulate the approach of the olefin to the reactive imido in **6b**. This increased bulk may well also further increase the overall catalytic rate.

Finally, we note that an imido mechanism like that mediated by half-sandwich catalysts **1** has been excluded for the related constrained geometry Zr catalysts **XII**.⁶⁰ A simple explanation for this difference in behavior would be that in **XII** the free coordination site allows migratory insertion and the relatively low steric profile does not tend to promote α -elimination to an imido species. A more subtle picture may emerge from computational studies.

Experimental Section

General Considerations. All manipulations were conducted using standard inert-atmosphere techniques using a dual-manifold argon/vacuum Schlenk line or an MBraun LabStar glovebox. All glassware and cannulas were stored in an oven at >373 K. Solvents were (where necessary) pre-dried over sodium wire and then refluxed under nitrogen and distilled from an appropriate drying agent—toluene from sodium; pentane and diethyl ether from NaK alloy; acetonitrile from CaH₂—stored in glass ampoules, and rigor-

ously degassed before use. C₆D₆ and toluene-*d*₈ were refluxed in vacuo for 3 days over potassium metal and vacuum-transferred before use. CDCl₃ was purchased from Aldrich and stored over 4 Å molecular sieves.

The salicyloxazoline proligands,^{73,74} Cp*Zr(NMe₂)₃⁷² and Cp*Zr(NHBUt)₃,⁸² and complexes **1a,c**, **4d,e**, and **5a,b**⁴⁵ were prepared according to published procedures. LiNMe₂ (99.9% grade) was purchased from Chemat Technology and used as received. The hydroamination substrates 1-amino-2,2-dimethylpent-4-ene (**2a**),⁸⁷ 1-amino-2,2-dimethylhex-5-ene (**3a**),³⁶ 1-amino-2,2-diphenylpent-4-ene (**2b**),⁸⁷ 1-amino-2,2-diphenylhex-5-ene (**3b**),⁸⁸ and 1-amino-2,2-dimethylhept-6-ene²³ were prepared according to literature procedures, dried for 3 days at ambient temperature over CaH₂, vacuum-transferred, and stored in a glovebox. 1-Amino-2,2-dimethylpent-4-ene-*d*₂ was prepared via a variation of the literature method,⁶⁰ using diethyl ether rather than dichloromethane as solvent. NMR tubes, including those for in situ reactions, were fitted with a J. Young PTFE concentric stopcock.

NMR spectra were recorded on Bruker DPX-400, AV-400, DRX-500, and AV III 600 spectrometers at 298 K unless otherwise stated. The spectra were internally referenced using the residual proton solvent resonance relative to tetramethylsilane ($\delta = 0$ ppm). Routine NMR assignments were confirmed by ¹H–¹H (COSY) and ¹³C–¹H (HMQC) correlation experiments where necessary. Elemental analyses were obtained by Warwick Analytical Services, Coventry, UK, and MEDAC Ltd., Surrey, UK.

Crystallography. A suitable crystal of **1b** was mounted on a glass fiber using an inert oil prior to transfer to a cold nitrogen gas stream and held at 100 K with an Oxford Cryosystems Cobra on an Oxford Diffraction Gemini four-circle diffractometer system with a Ruby CCD area detector using Mo K α radiation (= 0.71073 Å). Diffractometer control and data collection were done with a CrysAlis CCD (Oxford Diffraction, 2008). Data were collected with 1° frame exposures using ϕ and ω scans. Intensities were corrected semi-empirically for absorption, based on symmetry-equivalent and repeated reflections with CrysAlis RED (Oxford Diffraction, 2008). The structures were solved by direct methods using SHELXS (TREF)^{89,90} with additional light atoms found by Fourier methods. All non-hydrogen atoms were refined anisotropically. H atoms were placed at calculated positions and constrained with a riding model with *U*(H) set at 1.2 (1.5 for methyl hydrogens) times *U*_{eq} for the parent atom. SHELX97 was used for structure solution, refinement, and molecular graphics.⁹¹ Compound **1b**: (C₃₃H₅₅N₃O₂Zr)₂, *M* = 617.02, colorless block, 0.40 × 0.30 × 0.10 mm, monoclinic, space group *P*2₁/*c*, $\beta = 115.4160(10)^\circ$, *a* = 19.1703(2) Å, *b* = 9.71680(10) Å, *c* = 39.0199(6) Å, *V* = 6564.92(14) Å³, *Z* = 4, *D*_{calc} = 1.249 g cm⁻³, *T* = 100(2) K, with Mo K α (0.71073), 63 819 reflections measured, 12 294 unique (*R*_{int} = 0.0383), *R*1 [*I* > 2 σ (*I*)] = 0.0444, *wR*2 (*F*, all data) = 0.904, GoF = 1.018.

Complex Synthesis. [Cp*ZrL²(NMe₂)₂], **1b**. A Schlenk tube was charged with Cp*Zr(NMe₂)₃ (0.50 g, 1.4 mmol) and HL² (0.42 g, 1.4 mmol). Diethyl ether (30 mL) was added, and the reaction was stirred at ambient temperature for 16 h. The solution was filtered and concentrated to ca. 10 mL before the resultant precipitate was collected by filtration and dried in vacuo. Yield: 0.40 g, 47%. ¹H NMR (400 MHz, C₇D₈, 283 K): δ 0.85 (s, 3H, CH₃), 1.11 (s, 3H, CH₃), 1.36 (s, 9H, CMe₃), 1.72 (s, 9H, CMe₃), 1.81 (s, 15H, C₅Me₅), 3.01 (s, 6H, Zr-NMe₂), 3.40 (s, 6H, Zr-NMe₂), 3.44 (d, 1H, OCH₂ oxazoline, ²*J*_{HH} = 8 Hz), 3.53 (d, 1H, OCH₂ oxazoline, ²*J*_{HH} = 8 Hz), 7.68 (d, 1H, Ar C-H, ⁴*J*_{HH} = 3 Hz), 8.00 (d, 1H, Ar C-H, ⁴*J*_{HH} = 3 Hz) ppm. ¹³C{¹H} NMR (100.6 MHz, C₇D₈, 283

(87) Martinez, P. H.; Hultzsich, K. C.; Hampel, F. *Chem. Commun.* **2006**, 2221.

(88) Kondo, T.; Okada, T.; Mitsudo, T.-A. *J. Am. Chem. Soc.* **2002**, *124*, 186.

(89) Sheldrick, G. M. *Acta Crystallogr.* **1990**, *A46*, 467.

(90) Sheldrick, G. M. *Acta Crystallogr., Sect. A: Found. Crystallogr.* **2008**, *64*, 112.

(91) Sheldrick, G. M. *SHELX97*; Madison, WI, 1997.

K): δ 11.4 (C_5Me_5), 24.2, 28.6 ($NCMe_2$), 30.9, 31.7 (CMe_3), 34.3, 35.8 (CMe_3), 45.5, 49.0 ($Zr-NMe_2$), 69.9 ($NCMe_2$), 78.1 (OCH_2), 113.5 (Ar C_q), 119.7 (C_5Me_5), 124.1, 129.5 (Ar C-H), 137.9, 139.7, 165.8 (Ar C_q), 169.0 (C_q oxazoline). Anal. Calcd for $C_{33}H_{55}N_3O_2Zr$: C, 64.24; H, 8.98; N, 6.81. Found: C, 64.03; H, 8.82; N, 6.32. Single crystals of **1b** suitable for X-ray diffraction analysis were obtained from a saturated solution from diethyl ether at ambient temperature.

(Zr,S_C)-[Cp*ZrL¹(NH^tBu)₂], **1f**. An NMR tube was charged with **1a** (0.02 g, 0.03 mmol), ^tBuNH₂ (0.02 g, 0.3 mmol), and benzene-*d*₆ (0.6 mL). The yellow solution was analyzed by NMR spectroscopy. ¹H NMR (400 MHz, C₆D₆): δ 0.47 (br s, 16H, BuNH₂), 0.83 (t, 18H, CH₃ of excess amine, ³J_{HH} = 7 Hz), 0.86 (t, 3H, CH₃, ³J_{HH} = 7 Hz), 0.97 (t, 3H, CH₃, ³J_{HH} = 7 Hz), 1.10 (m, 4H, 2CH₂), 1.21 (m, 32H, 2CH₂ of excess amine), 1.35 (s, 9H, CMe₃), 1.45 (m, 2H, CH₂), 1.55 (m, 2H, CH₂), 1.71 (s, 9H, CMe₃), 1.95 (s, 15H, C₅Me₅), 2.05 (m, 1H, NHCH₂), 2.47 (br m, 16H, CH₂ of excess amine), 3.21 (m, 1H, NHCH₂), 3.47 (dd, 1H, NH, ³J_{HH} = 9 Hz, ³J_{HH} = 9 Hz), 3.59 (m, 2H, NHCH₂), 3.75 (dd, 1H, OCH₂ oxazoline, ²J_{HH} = 9 Hz, ³J_{HH} = 3 Hz), 4.04 (t, 1H, OCH₂ oxazoline, ²J_{HH} = 9 Hz, ³J_{HH} = 9 Hz), 4.71 (t, 1H, NH, ³J_{HH} = 8 Hz), 4.94 (dd, 1H, NCHPh oxazoline, ³J_{HH} = 9 Hz, ³J_{HH} = 3 Hz), 6.83 (m, 2H, Ar C-H of Ph), 6.91 (m, 3H, Ar C-H of Ph), 7.75 (d, 1H, Ar C-H, ⁴J_{HH} = 3 Hz), 8.09 (d, 1H, Ar C-H, ⁴J_{HH} = 3 Hz) ppm. ¹³C{¹H} NMR (100.6 MHz, C₆D₆): δ 11.4 (C_5Me_5), 14.1 (CH₃ and excess amine CH₃), 14.2 (CH₃), 20.3 (CH₂ and excess amine CH₂), 20.8 (CH₂), 30.5, 31.7 (CMe_3), 34.4, 35.8 (CMe_3), 36.5 (excess amine CH₂), 38.9 (HNMe₂), 39.0, 39.2 (CH₂), 42.3 (excess amine CH₂), 50.3, 50.6 (CH₂), 70.4 (NCHPh oxazoline), 74.9 (OCH₂ oxazoline), 111.1 (Ar C_q), 117.9 (C_5Me_5), 123.6, 126.0, 128.3, 129.2, 130.4 (Ar C-H), 137.6, 140.1, 142.8, 166.0 (Ar C_q), 170.9 (C_q oxazoline) ppm.

(Zr,S_C)-[Cp*ZrL²(NHCH₂CMe₂CH₂CH=CH₂)(NMe₂)-(PhPhOx)], **1g**. An NMR tube was charged with **1a** (0.02 g, 0.03 mmol), **2a** (0.003 g, 0.03 mmol), and benzene-*d*₆ (0.6 mL). The yellow solution was analyzed by NMR spectroscopy. ¹H NMR (400 MHz, C₆D₆): δ 0.09 (br s, 1H, HNMe₂), 1.01 (s, 3H, CH₃), 1.03 (s, 3H, CH₃), 1.38 (s, 9H, CMe₃), 1.73 (s, 9H, CMe₃), 1.97 (s, 15H, C₅Me₅), 2.05 (dd, 1H, CH₂, ²J_{HH} = 13 Hz, ³J_{HH} = 7 Hz), 2.20 (s, 6H, HNMe₂), 2.31 (dd, 1H, CH₂, ²J_{HH} = 13 Hz, ³J_{HH} = 7 Hz), 2.37 (s, 6H, Zr-NMe₂), 2.84 (t, 1H, NH, ³J_{HH} = 13 Hz), 3.29 (d, 1H, CH₂, ³J_{HH} = 12 Hz), 3.36 (d, 1H, CH₂, ³J_{HH} = 12 Hz), 3.72 (dd, 1H, OCH₂ oxazoline, ²J_{HH} = 9 Hz, ³J_{HH} = 3 Hz), 4.02 (t, 1H, OCH₂ oxazoline, ²J_{HH} = 9 Hz, ³J_{HH} = 9 Hz), 4.71 (dd, 1H, NCHPh oxazoline, ³J_{HH} = 9 Hz, ³J_{HH} = 3 Hz), 5.10 (m, 2H, CH=CH₂), 6.01 (m, 1H, CH=CH₂), 6.75 (m, 2H, Ar C-H of Ph), 6.91 (m, 3H, Ar C-H of Ph), 7.76 (d, 1H, Ar C-H, ⁴J_{HH} = 3 Hz), 8.16 (d, 1H, Ar C-H, ⁴J_{HH} = 3 Hz) ppm. ¹³C{¹H} NMR (100.6 MHz, C₆D₆): δ 11.4 (C_5Me_5), 25.0, 26.0 (CH₃), 30.4, 31.7 (CMe_3), 35.9, 36.1 (CMe_3), 38.9 (HNMe₂), 45.3 (CH₂), 45.4 (Zr-NMe₂), 61.0 (CH₂), 70.5 (NCHPh oxazoline), 75.2 (OCH₂ oxazoline), 111.1 (Ar C_q), 116.3 (=CH₂), 118.4 (C_5Me_5), 123.7, 126.6, 128.9, 129.3, 130.4 (Ar C-H), 137.0 (=CH), 137.5, 140.1, 142.8, 143.0, 165.7 (Ar C_q), 171.0 (C_q oxazoline) ppm.

(Zr,S_C)-[Cp*Zr(NMe₂)(PhPhOx)], **4a**. A J. Young ampule was charged with **1a** (0.32 g, 0.5 mmol). Toluene (10 mL) was added, and the resulting yellow solution was heated at 90 °C for 4 d. The reaction vessel was allowed to cool to ambient temperature and the volatiles were removed in vacuo. The yellow oily residue was dissolved in pentane and dried in vacuo to remove residual toluene, yielding the title compound as a pale orange microcrystalline solid:

0.26 g, 87%. ¹H NMR (400 MHz, C₇D₈): δ 1.13 (s, 9H, CMe₃), 1.57 (s, 9H, CMe₃), 1.85 (s, 15H, C₅Me₅), 2.78 (s, 6H, Zr-NMe₂), 3.89 (dd, 1H, OCH₂ oxazoline, ²J_{HH} = 10 Hz, ³J_{HH} = 8 Hz), 4.40 (dd, 1H, NCH oxazoline, ³J_{HH} = 10 Hz, ³J_{HH} = 8 Hz), 5.50 (t, 1H, OCH₂ oxazoline, ²J_{HH} = 10 Hz, ³J_{HH} = 10 Hz), 6.57 (d, 1H, Ar C-H, ³J_{HH} = 7 Hz), 7.08 (dd, 1H, Ar C-H, ³J_{HH} = 7 Hz, ³J_{HH} = 7 Hz), 7.17 (t, 1H, Ar C-H, ³J_{HH} = 7 Hz), 7.38 (d, 1H, Ar C-H, ³J_{HH} = 7 Hz), 7.68 (d, 1H, Ar C-H, ⁴J_{HH} = 3 Hz), 7.91 (d, 1H, Ar C-H, ⁴J_{HH} = 3 Hz) ppm. ¹³C{¹H} NMR (100.6 MHz, C₇D₈): δ 11.8 (C_5Me_5), 30.9, 32.1 ($NCMe_2$), 31.1, 31.9 (CMe_3), 36.2, 39.3 (CMe_3), 42.3 (Zr-NMe₂), 74.1 (OCH₂), 74.3 (NCH), 111.5 (Ar C_q), 119.3 (C_5Me_5), 121.7 (Ar C-H of metalated Ph), 123.9 (Ar C-H), 126.4, 126.9 (Ar C-H of metalated Ph), 130.5 (Ar C-H), 138.2, 140.7 (Ar C_q), 138.8 (Ar C-H of metalated Ph), 151.2, 166.1 (Ar C_q), 169.2 (C_q oxazoline), 189.8 (Zr-C_{Ar}) ppm. Anal. Calcd for $C_{35}H_{48}N_2O_2Zr$: C, 67.80; H, 7.80; N, 4.52. Found: C, 67.41; H, 7.33; N, 3.60.

[Cp*Zr(NMe₂)(Me₂PhOx)], **4b**. An NMR tube was charged with **1b** (0.02 g, 0.03 mmol) and benzene-*d*₆ (0.6 mL). The yellow solution was heated at 90 °C for 48 h and then analyzed by NMR spectroscopy. ¹H NMR (400 MHz, C₆D₆): δ 0.99 (s, 3H, CH₃), 1.20 (s, 3H, CH₃), 1.47 (s, 9H, CMe₃), 1.61 (s, 9H, CMe₃), 1.83, 1.90, 2.04, 2.09 (all s, 3H, 4 × CH₃ of Cp*), 2.19 (d, 6H, HNMe₂), 2.82 (s, 6H, Zr-NMe₂), 3.22 (d, 1H, Zr-CH₂, ²J_{HH} = 13 Hz), 3.54 (d, 1H, OCH₂ oxazoline, ²J_{HH} = 7 Hz), 3.55 (d, 1H, Zr-CH₂, ²J_{HH} = 13 Hz), 3.62 (d, 1H, OCH₂ oxazoline, ²J_{HH} = 7 Hz), 7.48 (d, 1H, Ar C-H, ⁴J_{HH} = 3 Hz), 8.19 (d, 1H, Ar C-H, ⁴J_{HH} = 3 Hz) ppm. ¹³C{¹H} NMR (100.6 MHz, C₆D₆): δ 10.1, 10.8, 11.0, 11.4 (C_5Me_4), 30.3, 31.7 ($NCMe_2$), 30.5, 32.2 (CMe_3), 35.7, 35.8 (CMe_3), 39.1 (HNMe₂), 41.8 (Zr-NMe₂), 40.6 (Zr-CH₂), 65.8 ($NCMe_2$), 77.8 (OCH₂), 104.6 (Ar C_q), 115.9, 116.4, 117.3, 119.1, 119.8 (C_5Me_4), 121.7, 123.0 (Ar C-H), 124.9, 136.5, 140.6 (Ar C_q), 169.3 (C_q oxazoline).

Hydroamination Procedure. The precatalyst (10 mg, 15–16 μ mol), substrate (18–38 mg, 150–160 μ mol), and internal standard, ferrocene (4 mg, 22 μ mol), were weighed into vials in a glovebox. Toluene-*d*₈ (600 mg, 0.64 mL) or THF-*d*₈ (634 mg, 0.64 mL) was used to mix the contents of the vials and transfer the solution to a J. Young NMR tube, which was sealed and shaken vigorously. NMR spectra at calibrated temperatures were recorded at appropriate intervals (typically 5–15 min), and the data processing and calculation of *N_i* were performed according to the method of Marks and co-workers.^{23,78}

Acknowledgment. We thank the EPSRC for financial support including an Advanced Research Fellowship for D.J.F. The Oxford Diffraction Gemini XRD system was obtained through the Science City Advanced Materials project: Creating and Characterising Next Generation Advanced Materials project, with support from Advantage West Midlands (AWM) and part funded by the European Regional Development Fund (ERDF).

Supporting Information Available: Kinetic, Eyring, and Arrhenius plots for hydroamination reactions; crystallographic data for **1b** in CIF format; NMR spectra of complexes. This material is available free of charge via the Internet at <http://pubs.acs.org>.

JA106588M